Molecular BioSystems

Accepted Manuscript

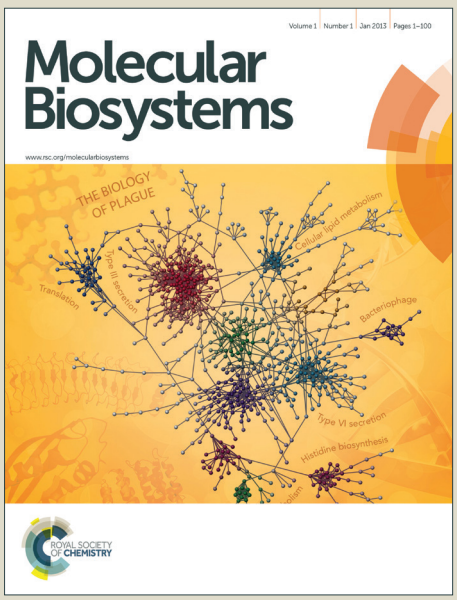

ROYAL SOCIETY OF CHEMISTRY

www.rsc.org/molecularbiosystems

Cite this: DOI: 10.1039/c0xx00000x

www.rsc.org/xxxxxx

ARTICLE TYPE

Synthesis and Protein Kinase C (PKC)-C1 Domain Binding Properties of Diacyltetrol Based Anionic Lipids

Narsimha Mamidi,‡ Subhankar Panda,‡ Rituparna Borah and Debasis Manna*

Received (in XXX, XXX) Xth XXXXXXXXX 20XX, Accepted Xth XXXXXXXXX 20XX

DOI: 10.1039/b000000x

Protein kinase C (PKC) family of lipid-activated kinases plays a significant role in the regulation of diverse cellular functions including tumor promotion, apoptosis, differentiation, and others. The lipophilic second messenger diacylglycerols (DAGs) acts as endogenous ligand for the PKCs in the presence of anionic phospholipids. To develop effective PKC regulators and understand the importance of anionic phospholipids in DAG binding of PKC isoforms, we conveniently synthesized octanoic acid containing diacyltetrol (DAT) based hybrid lipids with both DAG and anionic phospholipids headgroups within the same molecule. We also used palmitic and oleic acid containing hybrid lipids for additional understanding in PKC-C1 domain binding mechanism. Biophysical studies showed that hydrophobic side chains, DAG and anionic phospholipids headgroups, are necessary for their interaction with the C1-domain of PKC isoforms. The hybrid lipids DAT-PS and DAT-PA specifically interact with the PKCδ-C1b and PKCθ-C1b subdomains and showed 5- and 2.5-fold stronger binding affinity compare with DAG, respectively. Whereas, PKCα-C1a subdomain interacts with the hybrid lipids, without any significant specificity. The present results show that hybrid lipids bind to the PKC C1b/a subdomains and can be further studied to decipher their binding mechanism and biological activities. This study proposes a new concept of developing PKC activators by using tetrol-based anionic hybrid lipids having both phospholipids and diacylglycerol headgroups within the same molecule. This study also supplies useful information for the binding potencies of hybrid lipids with PKC-C1 domains.

Introduction

The diacylglycerol (DAG) mediated regulation of protein kinase C (PKC) family of serine/threonine kinases plays a critical role in several intracellular signaling pathways and the pathology of several diseases including cancer, neurological, cardiovascular, and others.[1-4] In consequence, PKC isoenzymes are being actively pursued as the subject of intense research and drug development. Depending on their enzymatic properties and activation mechanism, the mammalian PKC isoenzymes have been categorized into classical (calcium-, DAG-, and phospholipid-dependent), novel (calcium-independent, but DAG- and phospholipid-dependent), and atypical (calcium- and DAG-independent) subgroups.[1-5] The DAGs selectively interact with the C1 domain of PKC isoenzymes. This interaction induces their translocation to the discrete subcellular compartments. For some of the PKC isoenzymes, such translocation leads to activation. Detail mechanistic studies of PKC activation process shows that the cellular translocation of classical PKC isoenzymes to the plasma membrane is initially mediated by Ca^{2+} binding through C2 domain, followed by C1 domain-DAG interactions in the presence of anionic phospholipids. In contrast, only DAG binding to the C1 domain in the presence of anionic phospholipids activates novel PKC isoenzymes. DAG binding allows PKC isoenzymes to penetrate into the cellular membrane and folding-out an N-terminal pseudosubstrate region that permits admittance of a myriad of substrates to the catalytic site of the PKC isoenzymes.[4-9]

The C1 and C2 domains of PKC isoenzymes have strong binding affinities for anionic phospholipids, so it is difficult to use the whole-enzyme to characterize the role of anionic phospholipids in DAG binding affinity of PKCs. Previous studies also reported that the PKC-C1 domains have the determinants for the stereo-specific interaction of the anionic phospholipids, in particular the phosphatidylserine (PS).[5, 10, 11] On the other hand, the sizes of C1 domains are small; overall structures are highly conserved and there is DAG/ligand binding site. Several studies have already reported that the regulatory domain of PKCs may have independent biological activities. Consequently, C1 domains have become an attractive target in designing PKC ligands.[6, 12, 13] The regulatory domain of classical and novel PKC isozymes contains two functionally nonequivalent C1 domains; (C1a and C1b) positioned in tandem. The PKCα-C1a and PKCθ-C1b subdomains show higher DAG binding affinity in comparison with the C1b and C1a subdomain respectively. For PKCδ-C1b/a subdomains, conflicting results have been reported regarding their DAG binding affinity.[14]

Accumulating evidences suggest that anionic phospholipids including PS, phosphatidic acid (PA) and phosphatidylglycerol

(PG) enhance the DAG dependent membrane binding affinity and PKC activity; although the anionic phospholipids dependence varies considerably among the PKC isozymes.[10, 14] Phospholipids are essential component of cell membranes and contributes to the fluidity and stability of lipid bilayer. These conventional anionic lipids are also known to interact with the PKC-C1 domains through its positively charged binding pocket and enhance their DAG binding potencies and PKC enzyme activities. The reported DAG binding mechanism shows that the C1 domains first non-specifically interact with the membrane containing anionic lipids and then specifically binding with the DAG molecules.[4, 5, 15, 16] It is also documented that these conventional anionic lipids are specific activators of C1 domain containing PKC isoforms. For classical PKCs, PKCα and PKCβ$_{II}$ prefer PS to PG, whereas PKCγ shows comparable affinity for PS and PG.[11, 14, 17] Among the novel PKCs, PKCδ and PKCθ show a certain degree of PS selectivity, whereas PKCε shows preference for PA.[11, 14, 18, 19] Similar selectivity has been observed for the isolated C1b subdomains of PKCδ, PKCθ and PKCε. Whereas the PKCβII-C1b subdomain shows little preference between PS and PG. However, the reported experimental measurements either used DAG or a combination of separate DAG and anionic phospholipids molecules in solution or under liposomal environment to determine the DAG dependent membrane binding capabilities of the effectors proteins.[20, 21] Therefore, it is difficult to understand the role of both the lipid headgroups simultaneously in their effectors protein binding capabilities. It is also documented that cellular distribution of lipids including DAG and phospholipids are not homogeneous across the cellular membranes.[22] Whereas, presence of phospholipids is must for DAG dependent PKC activation through the C1 domains.[11, 23] Recent report also mentioned that only phospholipids can activate PKC enzyme through its interaction with the C2 domain.[24] A comparison of the membrane binding properties showed that the DAG binding affinity and specificity of the C1 domains increases with the increase in concentration of these anionic phospholipids from 5 mol % to 40 mol% (binding affinity increase by 40- fold under liposomal environment).[14] We hypothesize that hybrid lipids of these anioinic phospholipids and DAG can provide the ideal environment required for PKC activation. In addition, the modification of natural DAG structure, to attain higher membrane localization and activation of the targeted proteins in the presence of anionic lipids have been reported on several occasions, [25-29] surprisingly the design and synthesis of lipids having both DAG and anionic lipid headgroups within the same moiety have never been attempted. The hybrid lipids can form a stable bilayer (liposome) and provide the driving force for the formation of membrane-C1 domain complex.[26] Although the free rotations of separated lipid molecules get restricted in hybrid lipids but, hybrid lipids provide more stability to the liposomes.[30]

Recently diacyltetrol (DAT) lipids have been explored for the development of PKC modulator and biologically active lipid probes. The binding parameters of DAT-lipid with two hydroxymethyl groups (DAT-4) showed 3 to 4-fold stronger binding affinity in comparison with DAGs for PKCδ-C1b and PKCθ-C1b, respectively.[25] Our recent studies indicated that DAT-based anionic hybrid lipids interact with the PKCθ-C1b subdomain.[26] Therefore, to extend the utility of DAT based lipids as PKC modulators; in this article, we report the synthesis of three hybrid lipids with short chain length (DAT-PX$_8$, where PX = PA, PS, PG) and use of six other hybrid lipids, DAT-PX$_{16}$ and DAT-PX$_{18}$ with long chain lengths for detailed biophysical analysis. We characterized the binding affinities of these hybrid lipids with the isolated C1 domains of PKCδ, PKCθ and PKCα. The measure binding parameters showed that PKCδ-C1b and PKCα-C1a prefer DAT-PS and DAT-PA, respectively. Whereas, comparable binding affinity for all these hybrid lipids was observed for PKCα-C1b subdomain.

Results and Discussion

Design and Synthesis— We have recently reported a series of DAT based lipids as PKC-C1 domain regulators.[25] In our continued effort to develop improved PKC activators and understand the importance of anionic phospholipids in DAG/ligand binding, we selected DAT-1 lipid with the 1,4-diol moiety. The structural analysis clearly showed that one of the hydroxymethyl groups of DAT-1 lipid could be easily modified for further development of PKC regulators.[25, 26] The C1 domains of PKCs are reported to have anionic phospholipids dependent DAG binding affinity. So far, the anionic phospholipids dependencies in the DAG binding of the PKC-C1 domains were measured using separate molecules of DAG with PS/PA/PG phospholipids under liposomal environment. To measure C1 domain binding affinity for the hybrid lipids having both DAG and anionic lipid headgroup, we synthesized a family of DAT based hybrid lipids, where one molecule of hybrid lipid contains either PS- or PA- or PG- headgroup along with the DAG headgroup (Figure 1). Therefore, these hybrid lipids are structural mimic of the DAG and PS/PA/PG lipids. The hydrophobic interactions are difficult to model. Hence, we also used hybrid lipids with longer chain length to study the impact of different functionality and 'lipid tail' on the binding affinity. It has also been reported that, lipids with unsaturated acyl- groups are abundant in cellular membranes and more potent in PKC activation than the saturated ones.[31, 32] Consequently, we used hybrid lipids with unsaturated fatty acid (oleic acid).[26] The aim of this work was to study the binding properties of PKCα-C1a, PKCδ-C1b and PKCθ-C1b subdomains with the synthesized anionic hybrid lipids.

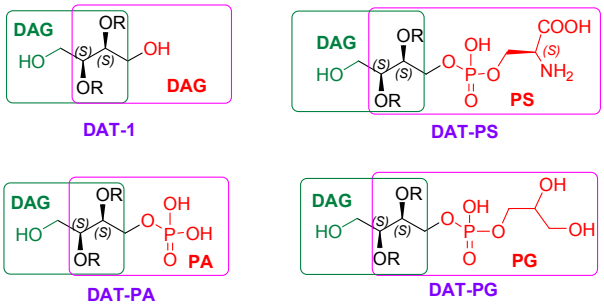

DAT-PA$_8$, DAT-PS$_8$, DAT-PG$_8$; R =CO(CH$_2$)$_6$CH$_3$
DAT-PA$_{16}$, DAT-PS$_{16}$, DAT-PG$_{16}$; R =CO(CH$_2$)$_{14}$CH$_3$
DAT-PA$_{18}$, DAT-PS$_{18}$, DAT-PG$_{18}$; R =CO(CH$_2$)$_7$(CH)$_2$(CH$_2$)$_7$CH$_3$

Figure 1: Structure of the hybrid lipids used for the present study.

The hybrid lipids were synthesized from (+)-diethyl L-tartrate. This C_2 symmetric starting material was used to avoid mixing of

enantiomeric products during synthesis. It is reported that the selection of stereochemistry of the lipid backbone is crucial as variety of stereochemistry of these structures confound the real specificity for the proteins. The (+)-diethyl-L-tartrate offers the stereochemistry as there in natural DAGs and anionic lipids at the *sn*-2 position. The hybrid lipids DAT-PX (where PX = PA, PS, PG) were synthesized in seven steps. DAT-PA_8 lipid was initially

Scheme 1: Synthetic route to DAT-PA lipids

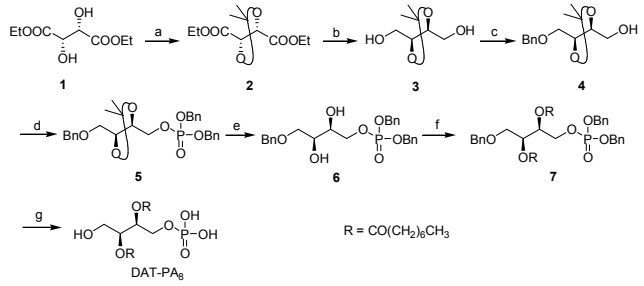

Reagents and conditions: (a) 2,2-dimethoxypropane, *p*-TsOH, toluene, Dean-Stark trap, 8 h, 84%; (b) $LiAlH_4$, THF, 0-65 °C, 7 h, 98%; (c) BnBr, Ag_2O, CH_2Cl_2, rt, 8h, 84%; (d) dibenzyl diisopropylphosphoramidite, 1*H*-tetrazole, rt, 4h, then *meta*-chloroperbenzoic acid, -20 °C to rt, 1 h, 92%; (e) *p*-TsOH, methanol, rt, 4 h, 82%; (f) octanoic acid, *N,N′*-dicyclohexylcarbodiimide, 4-dimethylaminopyridine, CH_2Cl_2, rt, 12 h, 86%; (g) 10% Pd-C, H_2 (80 psi), rt, 30 min, 90%.

synthesized to investigate the role of additional PA headgroup within the same molecule in binding with the PKC-C1 domains. We first prepared protected alcohol **4** from (+)-diethyl L-tartrate in three steps according to the reported procedures (Scheme 1).[25] The phosphate headgroup, protected as a phosphotriester, was then installed using dibenzyl diisopropylphosphoramidite to afford compound **5** in high yield (92%). Careful removal of the isopropylidene group under mild anionic conditions furnished diol **6** in 82% yield.[27, 28] The acyl chains were then introduced into the diol **6** using a standard *N,N′*-dicyclohexylcarbodiimide (DCC) mediated coupling reaction[25] with readily available caprylic acid to produce compound **7** in 86% yield. Finally, the benzyl groups were removed using catalytic amount of 10% Pd–C under hydrogenation conditions to access DAT-PA_8 in 90% yield.[26] We used DAT-PA_{16} with palmitic acid to study the impact of alkyl chain length on the binding affinity. To understand the role of unsaturated lipids in PKC-C1 domain binding, we also used DAT-PA_{18} with oleic acid.[26] Several research groups have extensively studied the PS dependency in the DAG binding of the PKC-C1 domains. To understand the importance of PS headgroup in the DAG binding of PKC-C1 domains, we synthesized DAT-PS_8 hybrid lipids from protected alcohol **4**. Initially, we attempted to synthesize **10** by directly installing protected PS headgroup onto protected alcohol **4**. However, removal of isopropylidene group under mild acidic environment led to a significant amount of hydrolysis of phosphotriester group. Thus, this approach was not feasible (Scheme 2). Therefore, we prepared **16** from protected alcohol **4** to optimize one-pot multicomponent reaction for the synthesis of DAT-PS_8 (Scheme 3). To avoid the problems associated with the hydrolysis of phosphotriester group, we focused on the development of a route in which isopropylidene group would be removed, prior to the installation of protected PS headgroup. For the efficient synthesis of DAT-PS_8, the diol **14** was prepared from protected alcohol **4** using TBDPS protection under basic condition, followed by careful removal of isopropylidene group under mild anionic condition.[27] The silylated diol **14** was subjected to a DCC-mediated coupling reaction with caprylic acid resulted **15** in 80-86% yield. The TBAF-assisted removal of TBDPS group furnished the key intermediate **16** in 98% yields. It is important to mention that the acyl- chain migration was not

Scheme 2: An attempted approach for the synthesis of DAT-PS/PG lipids

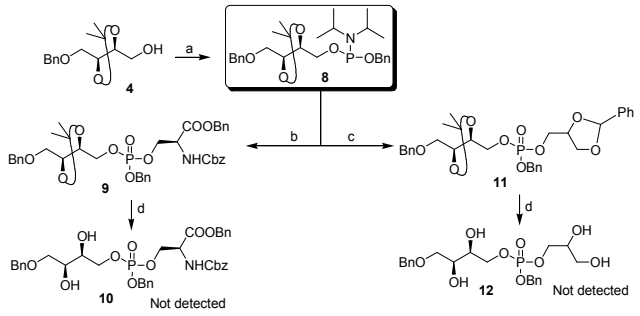

Reagents and conditions: (a) *O*-benzyl *N,N,N′,N′*-tetraisopropyl phosphoramidite, 1*H*-tetrazole, CH_2Cl_2, rt, 4h, 72%. (b) benzyl (S)-1-((benzyloxy)carbonyl)-2-hydroxyethyl carbamate/(2-phenyl-1,3-dioxan-4-yl)methanol, 1*H*-tetrazole, CH_2Cl_2, rt, 5 h then *meta*-chloroperbenzoic acid, -20 °C to rt, 1 h, 75%; (c) (2-phenyl-1,3-dioxan-4-yl)methanol, 1*H*-tetrazole, CH_2Cl_2, rt, 5 h then *meta*-chloroperbenzoic acid, -20 °C to rt, 1 h, 73%; (d) *p*-TsOH, methanol, rt, 4 h.

that significant (< 5% yield) for the conversion of compound **15** to **16**, under the experimental conditions. One-pot multicomponent phosphorylation reaction of protected alcohol **16**, protected serine and O-benzyl *N,N,N′,N′*-tetraisopropyl

Scheme 3: Synthetic route to DAT- PS/PG lipids

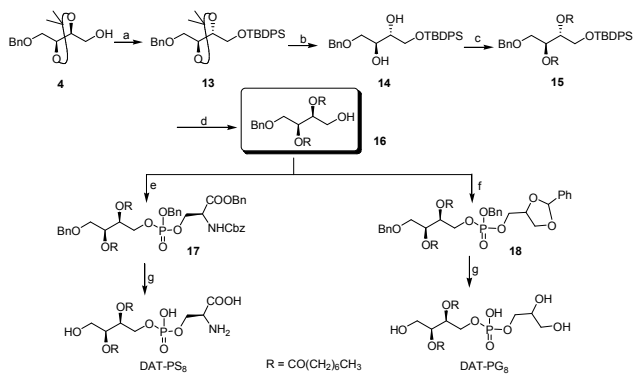

Reagents and conditions: (a) TBDPSCl, imidazole, 4-dimethylaminopyridine, dichloromethane, rt, 12 h, 98%; (b) *p*-TsOH, methanol, rt, 4 h, 85%; (c) octanoic acid, *N,N′*-dicyclohexylcarbodiimide, 4-dimethylaminopyridine, dichloromethane, rt, 12 h, 86%; (d) TBAF (solution 1.0 M in THF), 1 h, 98%; (e) *O*-benzyl *N,N,N′,N′*-tetraisopropyl phosphoramidite, 1*H*-tetrazole, benzyl (S)-1-((benzyloxy)carbonyl)-2-hydroxyethyl carbamate/(2-phenyl-1,3-dioxan-4-yl)methanol, 5 h, rt, then *meta*-chloroperbenzoic acid, -20 °C to rt, 1 h, 83%; (f) *O*-benzyl *N,N,N′,N′*-tetraisopropyl phosphorodiamidite, 1*H*-tetrazole, (2-phenyl-1,3-dioxan-4-yl)methanol, 5 h, rt, then *meta*-chloroperbenzoic acid, -20 °C to rt, 1 h, 83%; (g) 10% Pd-C, H_2 (80 psi), rt, 30 min, 90%.

phosphoramidite in the presence of 1*H*-tetrazole, followed by

oxidation using *meta*-chloroperbenzoic acid yielded phosphorylated compound **17**. Finally, the benzyl groups were removed using optimized catalytic hydrogenation reaction conditions, to access DAT-PS_8 in 90% yield.[26] We used DAT-PS_{16} and DAT-PS_{18} for further C1 domain binding analysis. Similarly, to understand the importance of PG headgroup in DAG binding of PKC-C1 domains, we prepared DAT-PG_8 hybrid lipid. The protected alcohol **11** was coupled with the 1,2-*O*-benzylidene glycerol, using one-pot phosphorylation reaction conditions to furnish intermediate **18** as shown in the scheme 3. The targeted 1,2-*O*-benzylidene glycerol was prepared from glycerol according to the reported procedures. Finally, the deprotection of benzyl groups under optimized catalytic hydrogenation reaction conditions provided DAT-PA_8 in 90% yield.[26] We also used DAT-PS_{16} and DAT-PS_{18} for further C1 domain binding analysis.

Extent of Membrane Localization of the Hybrid Lipids— The DAG and anionic lipid headgroups of the hybrid lipids are expected to be positioned near the bilayer/water interfacial region. However, the extent of localization of these headgroups at the bilayer/water interface is one of the indispensable criteria for their ability to interact with the PKC-C1 domains under the liposomal environment. Therefore, we measured sodium dithionite-induced NBD fluorescence quenching rates using DPPC/Ligand/NBD-PE liposomes. The NBD dye is embedded close to the interface, providing a useful marker for surface interactions of membrane-active C1 domain ligands.[33-35] It is necessary to emphasize that, the rate of sodium dithionite-induced NBD fluorescence quenching showed significant differences among the ligand-associated liposomes (Figure 2). The measured quenching rates suggest that, the NBD dye became more "shielded" from the soluble dithionite quencher, because of the presence of ligands in the liposomes. Therefore, perturbation of the membrane environment by these hybrid lipids may enhance the ability of molecules such as NBD and ultimately PKC-C1 domain to insert into the membrane. The results also imply that these ligands are more localized at the bilayer/water interface and more accessible for protein binding than DAG and DAT-**1a** are.

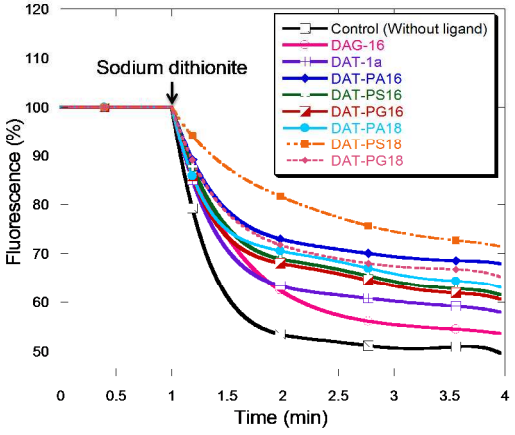

Figure 2: Fluorescence quenching of NBD-PE embedded in PC/ligand/NBD-PE (44.5:44.5:10:1) liposomes. Sodium dithionite, 0.6 µM; control, without ligand.

Measurement of change in bilayer fluidity induced by the hybrid lipids—To understand the consequences of hybrid lipids upon the dynamics of lipids and fluidity of the lipid bilayer we determined the fluorescence anisotropy of 1,6-phenyl-1,3,5-hexatriene (DPH) under liposomal environment. DPH is widely used as a probe to measure the change in dynamics of its lipid environment. The DPH molecules generally embedded within the hydrophobic core of the lipid bilayer therefore changes in fluorescence anisotropy values can be useful in evaluating the modulation of lipid-bilayer fluidity induced by membrane-active compounds.[35] Figure 3 represents the change in anisotropy values of DPH molecules in the presence of anionic hybrid lipids under liposomal environment. The variations in fluorescence anisotropy affected by the different anionic lipids are very small, but follow a certain pattern. The animosity values of DPH in the presence of unsaturated hybrid lipids (DAT-PX_{18}) are slightly smaller than that in the presence of saturated hybrid lipids (DAT-PX_{16}), indicating an enhanced bilayer fluidity.

Measurement of Protein Binding Parameters— Structural and functional studies of the PKC-C1 domains have revealed that Thr-12, Leu-21, and Gly-23 residues play a crucial role in DAG binding.[2, 36-38] The hydrophobic residues present along the

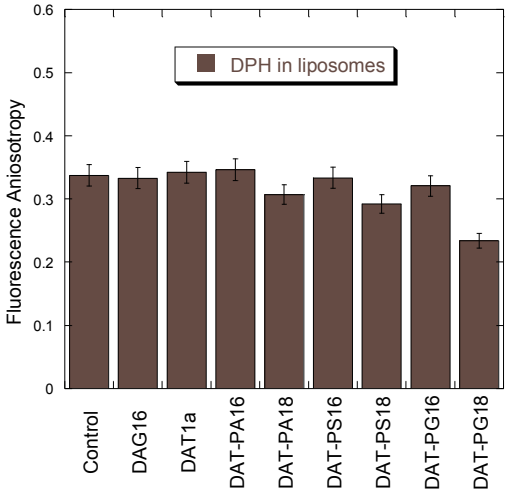

Figure 3: Fluorescence anisotropy of DPH embedded in PC/PE/PS (60/20/20) liposomes for DAG_{16} and DAT1a (2.9 µM) and PC/PE (80/20) liposomes for DAT-$PX_{16/18}$ lipids (2.9 µM). Control: no ligand was added to the liposomes.

circumference of the binding pocket facilitates the insertion of the C1 domain into the membrane after DAG binding, thereby stabilizing the formation of the ternary (ligand-receptor-membrane) binding complex. Their membrane interaction is also facilitated by a ring of positively charged residues located around the middle of the domain that potentially interact with the anionic phospholipids like PS, PA, or PG (Figure 4).[10-12, 14] These interactions are also important for binding with extrinsic proteins, including, Aβ-peptides, phospholipases, cytochrome-c and others. The PKC-C1a/b subdomains are known to have sufficiently strong binding affinity for DAG in the presence of anionic phospholipids. In this study, first the binding properties of the synthesized anionic lipids with these C1 domains were measured in monomeric form by using intrinsic fluorescence quenching

method and steady state fluorescence anisotropy measurements. Förster resonance energy transfer (FRET)-based competitive binding assay under liposomal environment was also used to measure their ligand binding affinities and specificities.[25, 33, 34]

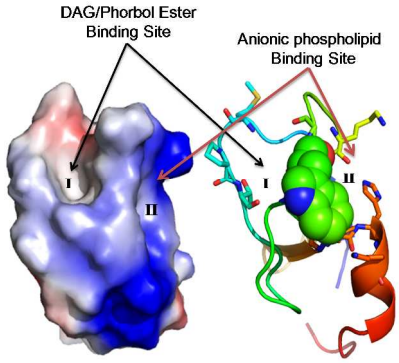

Figure 4: Structure of PKCδ-C1b subdomain (1PTR). The arrows indicate the DAG/phorbol ester and anionic phospholipid binding sites. I and II indicate the ligand binding sites of the PKCδ-C1b subdomain.

Interaction with Soluble Ligands— Fluorescence spectroscopy is a useful technique to detect ligand-induced change in protein conformation or microenvironment. The intrinsic fluorescence of the PKC-C1b/a subdomains is due to the presence of a single tryptophan (Trp-22), phenylalanine and tyrosine residues. The Trp-22 residue is also present close to the DAG binding pocket of the C1b/a subdomains of PKCδ, PKCθ and PKCα. The ability of the proteins to bind ligands in monomeric form was calculated from the ligand-induced Trp-fluorescence quenching data (Figure S1). The calculated values showed that the hybrid lipids with different chain length interact with the C1b/a subdomain with highest binding affinity (1.49—2.07 μM) and other lipids with comparable binding affinities for all three proteins (Figure S2). We have recently reported that, the DAT-**1** with two hydroxymethyl groups compared to one in DAG showed ~2-fold stronger binding affinity for PKCδ-C1b subdomain.[25] An interesting finding was the pivotal role played by the hybrid lipids in the binding of the C1b/a subdomains. The results showed that PKCδ-C1b subdomain has 5-fold stronger binding affinity for DAT-PS_8 than DAG_8. The other anionic hybrid lipid, DAT-PA_8 showed ~2-fold stronger binding affinity, whereas, DAT-PG_8 did not show any substantial preference for PKCδ-C1b subdomain than DAG_8. In the case of PKCθ-C1b subdomain, although DAT-PA_8 showed 2.5-fold stronger binding affinity than DAG_8, but there was no considerable differences in binding potencies for all the three hybrid lipids. Whereas, no significant preference for the hybrid lipids was observed for PKCα-C1a subdomain. To understand the importance of hydrophobicity of the ligands in C1-domain binding, a similar analysis was performed with the long chain hybrid lipids. All three proteins showed similar patterns of dependence on the hydrophobicity of the compounds (Table 1). For DAT-PX_8 and DAT-$PX_{16/18}$ (PX stands for PA, PS or PG) ligands, although there is a distinct difference in hydrophobicity, but the differences in binding affinities are small for all three proteins. This could be due to the binding orientations of proteins with the ligands. The overall higher binding affinity of the long chain hybrid lipids presumably due the interaction of long chains with the hydrophobic amino acids, surrounding the binding pocket of the C1 domains. Therefore, binding affinities of the hybrid lipids highlight the importance of ligand hydrophobicity and binding orientation.

Steady-state fluorescence anisotropy measurements of the proteins suggest that the presence of the ligands in monomeric form increases the rigidity of the surrounding environment of the protein in a manner similar to that of DAGs (Table S1). Therefore, the increases in anisotropy values of the proteins in the presence of the ligands also support their ligand binding properties.

Interaction with Ligand-Associated Liposomes— PKC isoenzymes are reported to interact with the membrane through their lipid-binding C1 and C2 domains. The PKC-C1 domains have both a membranes binding surface and a lipid-binding groove. The binding properties of the isolated C1 domains with the ligands under liposomal environment were quantitatively measured by protein-to-membrane FRET-based binding assay.[33, 34] The Trp residue of the PKC-C1b/a subdomains serve as the FRET donor, and a low density of membrane-embedded, dansyl-PE (dPE) lipids serve as the acceptors. DAG_8 was titrated into the solution containing C1b/a-subdomain-bound liposomes. The decrease in the protein-to-membrane FRET signal (Figure S3) was monitored to measure the displacement of protein from the liposomes surface to the bulk solution, and apparent inhibitory constant [$K_I(DAG_8)_{app}$] calculation. Figure 5 represents DAG_8 promoted displacement of PKCδ-C1b subdomain from ligand associated liposomes (PC/PE/dPE/DAT-PX_{16}). The values of $K_I(DAG_8)_{app}$ depend on ligand concentration and the background lipid composition in the liposomes as well as the affinities of the C1b/a subdomains for ligands/DAG_8. This assay showed that the

Table 1. K_D (ML) values for the binding of ligands with the PKCδ-C1b, PKCθ-C1b, and PKCα-C1a proteins[a] at room temperature.

Compound	*K_D (ML) (μM)*		
	PKCδ-C1b	PKCθ-C1b	PKCα-C1a
DAG_8	12.41 ± 0.59	6.74 ± 0.54	14.58 ± 0.44
DAT-**1b**	5.85 ± 0.48	4.83 ± 0.36	8.78 ± 0.41
DAT-PA_8	5.35 ± 0.23	2.53 ± 0.26	5.98 ± 0.34
DAT-PS_8	2.47 ± 0.21	2.70 ± 0.17	8.85 ± 0.45
DAT-PG_8	8.89 ± 0.43	3.27 ± 0.22	5.58 ± 0.28
DAG_{16}	7.04 ± 0.43	6.35 ± 0.37	8.31 ± 0.23
PA_{16}	9.43 ± 0.45	—	—
PS_{16}	7.72 ± 0.57	—	—
PG_{16}	8.54 ± 0.62	—	—
DAG_{16} + PA_{16} (1:1)	6.43 ± 0.45	—	—
DAG_{16} + PS_{16} (1:1)	3.01 ± 0.35	—	—
DAG_{16} + PG_{16} (1:1)	6.44 ± 0.48	—	—
DAT-**1a**	4.31 ± 0.25	3.89 ± 0.30	6.85 ± 0.11
DAT-PA_{16}	4.26 ± 0.21	2.07 ± 0.10	5.46 ± 0.34
DAT-PS_{16}	1.84 ± 0.17	2.27 ± 0.19	5.66 ± 0.23
DAT-PG_{16}	5.34 ± 0.22	2.63 ± 0.31	4.83 ± 0.38
DAT-PA_{18}	3.23 ± 0.19	1.49 ± 0.11	4.66 ± 0.51
DAT-PS_{18}	1.60 ± 0.11	1.70 ± 0.18	5.54 ± 0.43
DAT-PG_{18}	4.26 ± 0.31	2.24 ± 0.12	4.52 ± 0.34

[a] Protein, 1 μM in buffer (20 mM Tris, 160 mM NaCl, 50 μM $ZnSO_4$, pH 7.4). Values represent the mean ± S.D. from triplicate measurements.

Compound	$K_I(DAG_8)_{app}$ (μM)			$K_D(L_{16/18})$ (nM)		
	PKCδ-C1b	PKCθ-C1b	PKCα-C1a	PKCδ-C1b	PKCθ-C1b	PKCα-C1a
DAT-**1a**	17.14 ± 1.21	23.08 ± 2.48	9.68 ± 1.32	883.50 ± 11.23	533.13 ± 12.26	6365.90 ± 33.23
DAT-PA_{16}	20.59 ± 1.90	41.81 ± 3.23	15.38 ± 1.38	686.08 ± 11.87	136.99 ± 8.94	1447.56 ± 39.32
DAT-PA_{18}	29.88 ± 3.23	46.95 ± 5.89	15.46 ± 1.80	318.75 ± 8.72	86.20 ± 4.34	1134.79 ± 23.27
DAT-PS_{16}	43.65 ± 2.65	32.88 ± 2.95	10.34 ± 1.83	115.74 ± 7.86	195.04 ± 8.91	3186.72 ± 29.21
DAT-PS_{18}	46.26 ± 4.24	34.72 ± 3.05	11.36 ± 2.55	94.22 ± 6.89	135.40 ± 10.09	2503.47 ± 28.12
DAT-PG_{16}	14.33 ± 7.67	22.73 ± 1.91	19.52 ± 1.57	1562.20 ± 14.17	344.12 ± 15.29	864.73 ± 19.23
DAT-PG_{18}	14.74 ± 1.99	23.17 ± 1.86	22.18 ± 2.21	1062.98 ± 25.89	281.47 ± 9.81	673.14 ± 4.29

[a] Protein, 1 μM in buffer (20 mM Tris, 150 mM NaCl, 50 μM $ZnSO_4$, pH 7.4).
[b] Active liposome composition, PC/PE/PS/dPE/DAT-**1a** (55/15/20/5/5)
[c] Active liposome composition, PC/PE/dPE/$Ligand_{16/18}$ (75/15/5/5).

synthesized hybrid lipids interact with the C1 domains under liposomal environment. The results also showed that higher concentration of DAG_8 was required for the displacement of PKCδ-C1b protein from the DAT-$PS_{16/18}$ associated liposomes. The PKCθ-C1b subdomain showed highest binding affinity for DAT-$PA_{16/18}$ associated liposomes. Whereas, PKCα-C1a subdomain showed slight preference for DAT-$PG_{16/18}$ lipids. Finally, the equilibrium dissociation constant ($K_D(L_{16/18})$) for the

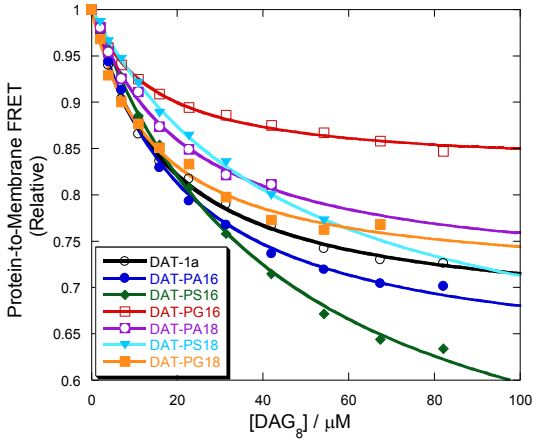

Figure 5: Competitive displacement assay for the PKCδ-C1b subdomain (1 μM) bound to liposome containing ligands DAT-1a (○), DAT-PA_{16} (●), DAT-PS_{16} (♦), DAT-PG_{16} (□), DAT-PA_{18} (◘), DAT-PS_{18} (▼), DAT-PG_{18} (■). Active liposome composition, PC/PE/dPE/$Ligand_{16/18}$ (75/15/5/5). The bound complex was titrated with the DAG_8.

C1b/a subdomains binding to the liposome-associated targeted ligand was calculated using equation 4. Comparison of the equilibrium dissociation constant also revealed that PKCδ-C1b and PKCθ-C1b subdomains have higher binding affinity for the DAT-$PS_{16/18}$ and DAT-$PA_{16/18}$ associated liposomes, respectively (Table 2). From the binding affinity results, it can be concluded that PKCδ-C1b, PKCθ-C1b and PKCα-C1a showed different binding affinities depending on the anionic phospholipids headgroup present in the hybrid lipids. These results validate that not only DAG but also anionic phospholipids are crucial for binding of the C1 domains to the membrane. The hybrid lipids, DAT-PX showed stronger binding affinities for the C1 domains compared to only DAG, PS, PA, or PG_{16} lipids. This indicates that isolated PKC-C1 domains may first interact with the anionic lipids due to electrostatic interaction and then strongly interacts with the DAG through hydrogen bond formation.

A comparison of the binding parameters observed for DAT-$PX_{16/18}$ led to the conclusion that all the three C1 domains have lower binding affinities for DAT-PX_{16} hybrid lipids. This could be due to the more fluidic state of the DAT-PX_{18} containing liposomes under the experimental condition. The fluidity of the membrane has been shown to be significant in determining the functioning of the PKC isoenzymes. It is reported that activity of the PKCα enzyme primarily depends on the membrane fluidity over the chain length and degree of unsaturation of the DAGs.[39, 40] We presume that, the fluidity formulates more loosely packed bilayers that allow the hydrophobic residues of the C1 domains to penetrate into the hydrophobic core of the lipid bilayer, which is essential for the PKC enzyme activation.[41, 42] Another intriguing finding was the substantial differences in the binding affinity between hybrid lipids and 1:1 lipid mixture of DAG with anionic phospholipids. There are reports on plausible Trp fluorescence quenching by the anionic phospholipids, due to their ability to donate a proton from the phosphate ion to the indole chromophore.[43, 44] Detailed structural analysis showed that the Trp residue present close to both the DAG/phorbol ester and anionic phospholipids binding sites (I and II, Figure 2). However, comparative protein binding measurements between 1:1 lipid mixture of DAG with anionic phospholipids and hybrid lipids clearly indicate that, the hybrid lipids have a certain degree of preference for the C1 domain, under the experimental conditions. We have also reported their C1 domain binding properties by using SPR analysis.[26] This real-time analysis also showed that the PKCθ-C1b subdomain has sufficiently strong binding affinity for these hybrid lipids and their binding pattern is in good correlation with the DAG only.

All these measured binding parameters either indicate that the hybrid lipids bind to the DAG/phorbol ester-binding site or with the positively charged residues located around the C1 domain. However, these binding parameters do not point out the genuine binding site of the C1 domain for the hybrid lipids. To identify the actual binding site of the hybrid lipid within the C1 domain, we performed molecular docking analysis to both the possible binding sites (I and II, Figure S4). Theoretical binding energy for each conformation and distribution of ligands between the two sites showed that these hybrid lipids bind to both the site with little preference for anionic lipid binding site (Figure 6 and Figure S5). Therefore, all these measurements indicate that the binding

of these hybrid lipids binding to PKC C1 domain follows a critical mechanism. These lipids (i) either can bind to the DAG/phorbol ester binding site (I) and shows Trp fluorescence quenching due to its displacement from hydrophobic environment to aqueous environment, or (ii) bind to the anionic lipid binding site (II) and quench Trp fluorescence due to transfer of proton from phosphate to indole chromophore and subsequent DAG_8 binding to the site (I) can cause a conformational change leading to the displacement of protein from membrane surface.

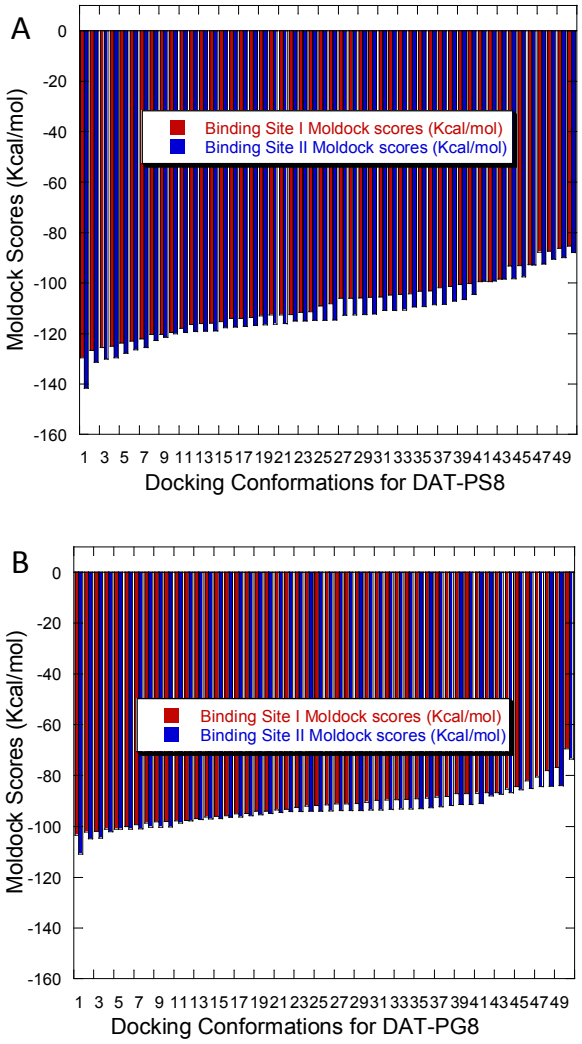

Figure 6: Theoretical binding energy calculation and distribution of DAT-PS_8 (A) and DAT-PG8 (B) between the DAG/phorbol ester binding site (I) and anionic lipid-binding site (II) of the PKCδ-C1b subdomain (1PTR).

Hence, measured binding parameters showed that the DAT based hybrid lipids interact differentially with C1b/a subdomains of PKCδ, PKCθ and PKCα, both in the monomeric form and under liposomal environment. Modifications of the acyl chain length showed a modest effect on the binding affinity. However, modification of headgroup of DAT based lipids showed a strong effect on the binding. Overall, these results validate that not only DAG but also anionic phospholipids are crucial for binding of the C1 domains to the membranes and long chain hybrid lipids can differentially influence the in vitro membrane interaction properties of the PKCδ, PKCθ, and PKCα. The hybrid lipid-C1 domain binding is driven by both electrostatic interaction and hydrogen bond formation. However, it is important to emphasize that the hybrid lipid specificity of the C1 domains is not in accordance with the reported anionic lipid specificity, measured using isolated DAG and anionic phospholipids. The specificity and binding affinity difference among the three proteins could be due to the difference in the interacting residues and areas of the activator-binding sites. The binding results also show that these compounds have higher binding affinity for PKCθ-C1b than for PKCδ-C1b and PKCα-C1a, possibly because of the additional hydrogen bonds. The results clearly indicate these lipids can be used as isoform specific PKC regulators. The molecular docking analysis indicate that the hybrid lipids can interact with the C1 domain through both DAG/phorbol ester binding site and anionic phospholipid binding site with slight preference for the second one. Currently, we are performing further studies, including PKC activity assay, cellular translocation measurements and others to understand their detail C1 domain-binding mechanism. However, the relative binding parameters clearly showed that these hybrid lipids bind to the C1 domains and presence of additional anionic lipid headgroup within the same molecule enhanced the C1 domain binding affinity and specificity of the hybrid lipids. In addition to this PKC activity measurements in signal transduction pathways its possible role in various diseases including Alzheimer's, inflammation, diabetes stroke, HIV and heart failure and other. PKC dependent cell signalling pathways are associated with such diseases. These hybrid lipids with anionic headgroup can also be used in liposome based controlled drug delivery, gene delivery methods and others.

Conclusion

This report described the detailed synthesis of a family of distinctive hybrid lipids and their binding measurements with the PKC-C1 domains. These tetrol based hybrid lipids with long (palmitic acid and oleic acid) and short chain (octanoic acid) fatty acids were synthesized from (+)-diethyl-L-tartrate. Syntheses of these hybrid lipids from the scratch afforded the ability to generate pure samples of a single lipid structure and freedom to explore the role of hydroxymethyl group and anionic lipid headgroups in protein binding. These hybrid lipids are structural mimic of DAG and anionic phospholipids having both DAG and anionic phospholipid headgroups within the same molecule. These lipids interact with the PKC-C1 domain in an isoform-specific manner and the presence of anionic lipid headgroup plays a significant role in their binding properties. PKCδ-C1b specifically interacts with DAT-PS lipid, whereas, PKCθ-C1b and PKCα-C1a prefers DAT-PA and DAT-PG to the other lipids. Membrane fluidity and air/water interfacial localization plays an important role for their binding potencies. However, their C1 domain binding mechanism is complex and can interact through either hydrophobic pocket or cationic groove. The results also reveal that both electrostatic and hydrophobic interactions play an important role of PKC C1 domain binding. This also makes these hybrid lipids as potential regulator of PKC isoenzymes and can be further developed as research tools or lead compound in drug

development. This study should help account for different cellular function and regulation capabilities of the proteins in which both DAG and anionic phospholipid binding sites resides.

Experimental Section

General Information: All reagents were purchased from Sigma (St. Louis MO) and Merck (Mumbai, India) and used directly without further purification. Dry solvents were obtained according to the reported procedures. Column chromatography was performed using 60—120 mesh silica gel. Reactions were monitored by thin-layer chromatography (TLC) on silica gel 60 F254 (0.25 mm). ^{1}H NMR, ^{13}C NMR, and ^{31}P NMR spectra were recorded at 400, 100, and 162 MHz, respectively using a Varian AS400 spectrometer. Coupling constants (*J* values) are reported in hertz, and chemical shifts are reported in parts per million (ppm) downfield from tetramethylsilane using residual chloroform (δ = 7.24 for ^{1}H NMR, δ = 77.23 for ^{13}C NMR) as an internal standard. ^{31}P NMR spectra were recorded in $CDCl_3$ and calibrated to external standard 85% H_3PO_4. Multiplicities are reported as follows: s (singlet), d (doublet), t (triplet), m (multiplet), and br (broadened). Melting points were determined using a melting point apparatus and are uncorrected. Mass spectra were recorded using a Waters Q-TOF Premier mass spectrometry system, and data were analyzed using the built-in software. Optical rotation values were measured at room temperature on a Perkin-Elmer 343 polarimeter. 1,2-Dipalmitoyl-*sn*-glycerol (DiC_{16}), 1,2-dioctanoyl-*sn*-glycerol (DiC_8), 1,2-dipalmitoyl-*sn*-glycero-3-phospho-L-serine (DPPS), 1,2-dipalmitoyl-*sn*-glycero-3-phosphate (DPPA), 1,2-dipalmitoyl-*sn*-glycero-3-phospho-(1'-*rac*-glycerol) (DPPG), 1,2-dioleoyl-*sn*-glycero-3-phosphoethanolamine-N-(5-dimethylamino-1-naphthalenesulfonyl) (NBD-PE), *N*-[5-(dimethylamino)naphthalene-1-sulfonyl]-1,2-dihexadecanoyl-*sn*-glycero-phosphoethanol -amine (Dansyl-PE) were purchased from Avanti Polar Lipids (Alabaster, AL). Ultrapure water (Milli-Q system, Millipore, Billerica, MA) was used for the preparation of buffers.

Synthesis of Anionic hybrid Lipids

General Procedure for the Deprotection of Isopropylidene Group (I): To a stirring solution of isopropylidene-protected compounds (1.0 equiv) in methanol (5 mL), *p*-TsOH (0.1 equiv) was added and stirring was continued at room temperature for 4 h. After completion of the reaction (monitored by TLC), the solvent was removed under reduced pressure to yield a residue. The residue was further dissolved in dichloromethane (10mL) and washed with a saturated solution of sodium bicarbonate (3×). The organic layer was dried over anhydrous Na_2SO_4 and concentrated under reduced pressure. Purification by silica gel column chromatography and a gradient solvent system of 20–30% ethyl acetate to hexane yielded diol derivatives.

General Procedure for the Preparation of Esters (II): Caprylic acid (2.2 equiv), *N,N'*-dicyclohexylcarbodiimide (2.2 equiv) and 4-dimethylaminopyridine (0.1 equiv) was added to a solution of protected alcohol (1.0 equiv.) in anhydrous dichloromethane (5 mL), under a N_2 atmosphere. Stirring was continued for 12 h at room temperature. After completion of the reaction, the reaction mixture was filtered and washed (3×) with dichloromethane. The filtrate was concentrated under reduced pressure, and the column chromatography was performed with silica gel, and a gradient solvent system of 2–5% ethyl acetate to hexane to yielded corresponding esters.

General Procedure for the Deprotection of Benzyl Groups (III): To a solution of benzyl ether containing compounds (1.0 equiv) in 10 mL of ethyl acetate/ethanol (3:1 ratio) was added 10% Pd–C catalyst (0.1 equiv) and stirring was continued under a H_2 (80 psi) atmosphere at room temperature for 30 min. After completion of the reaction, the catalyst was filtered through a pad of celite and washed with 30 mL of MeOH. Removal of solvent under reduced pressure yielded the targeted compounds.

General Procedure for the Deprotection of TBDPS Group (IV): To a stirring solution of TBDPS protected compound (1.0 equiv) in THF (5.0 mL) was added commercially available TBAF (2.0 equiv, 1.0 M solution in THF) at room temperature and stirring was continued for 1 h. After completion of the reaction, the solvent was removed under reduced pressure to yield a residue. The residue was dissolved in EtOAc (20 mL) and washed with a saturated solution of sodium bicarbonate (3×). The organic layer was dried over anhydrous Na_2SO_4 and concentrated under reduced pressure. Column chromatography with silica gel and a gradient solvent system of 7–10% ethyl acetate to hexane yielded alcohol derivatives.

General Procedure for the One-pot Phosphorylation of protected Alcohols to Prepare DAT-PS and DAT-PG derivatives (V): To an ice-cooled stirring suspension of *O*-benzyl *N,N,N',N'*-tetraisopropyl phosphoramidite (1.1 equiv) and 1*H*-tetrazole (6.0 equiv), protected alcohol (1.0 equiv) in anhydrous dichloromethane (2 mL) was added under N_2 atmosphere. After continuous stirring for 30 min benzyl, (S)-1-((benzyloxy)carbonyl)-2-hydroxyethylcarbamate or (2-phenyl-1,3-dioxan-4-yl)methanol (1.0 equiv) in anhydrous dichloromethane (2 mL) was added. The reaction mixture was stirred for another 5 h at room temperature and cooled to -20 °C, and a solution of *meta*-chloroperbenzoic acid (1.5 equiv) in dichloromethane (2 mL) was added. Finally, the reaction mixture was stirred for 1 h at room temperature, diluted with dichloromethane (30 mL), washed (3×) with 10% aqueous $NaHCO_3$ (10 mL) and brine (10 mL). The organic layer was dried over anhydrous Na_2SO_4 and concentrated under reduced pressure. Column chromatography with silica gel and a gradient solvent system of 27–30% ethyl acetate to hexane yielded corresponding phosphates compound.

Synthesis of (((4S,5S)-5-((benzyloxy)methyl)-2,2-dimethyl-1,3dioxolan-4-yl)methoxy)(*tert* butyl)diphenylsilane (8): To an ice-cooled stirring solution of *tert*-butylchlorodiphenylsilane (TBDPS-Cl, 340 µL, 1.31 mmol) in anhydrous dichloromethane (5 mL) were added triethylamine (182 µL, 1.31), catalytic amount of DMAP (15 mg, 0.12 mmol), and a solution of protected alcohol **4** (300 mg, 1.19 mmol) in dry dichloromethane (5 mL). The resulting mixture was allowed to warm up to room temperature and stirring was continued for 12 h at room

temperature. After completion of the reaction, the solvent was removed under reduced pressure. The residue was dissolved in dichloromethane (20 mL) and washed with a saturated solution of $NaHCO_3$. The organic layer was dried over anhydrous Na_2SO_4, and the solvent was removed under reduced pressure. Column chromatography with silica gel and a gradient solvent system of 3–5% ethyl acetate to hexane yielded **8** (572 mg, 98%).

Characterization of the synthesized compounds:

(2S,3S)-4-(benzyloxy)-1-{[bis(benzyloxy)phosphoryl]oxy}-3-(octanoyloxy)butan-2-yl octanoate (7): Using the general procedure (II), starting from compound **6** (100 mg, 0.212 mmol) compound **7a** (132 mg, 86%) was isolated as colorless oil. $[\alpha]^{20}_D$ = -20.3 (c 0.2, CH_2Cl_2); ^{1}H NMR (400 MHz, $CDCl_3$): δ_{ppm} 7.35-7.25 (m, 15H), 5.37-5.34 (m, 1H), 5.29-5.25 (m, 1H), 5.04-4.98 (m, 4H), 4.45 (d, 2H, J = 6.4 Hz), 4.20-4.15 (m, 1H), 4.11-4.04 (m, 1H), 3.57-3.49 (m, 2H), 2.29 (t, 2H, J = 7.6 Hz), 2.22 (t, 2H, J = 7.8 Hz), 1.64-1.53 (m, 4H), 1.16 (br s, 16H), 0.87 (t, 6H, J = 6.2 Hz); ^{13}C NMR (100 MHz, $CDCl_3$): δ_{ppm} 172.8, 172.7, 137.6, 135.7, 128.6, 128.5, 128.0, 127.9, 127.8, 127.7, 73.3, 70.1, 69.9, 69.5, 67.9, 65.7, 34.2, 34.1, 31.7, 29.1, 29.0, 24.9, 24.8, 22.6, 14.1; ^{31}P NMR (161.9 MHz, $CDCl_3$): δ_{ppm} 0.09; HRMS (ESI) Calcd for $C_{41}H_{57}O_9PNa^+$ $[M+Na]^+$: 747.3638, Found:.747.3637.

[(2S,3S)-4-hydroxy-2,3-bis(octanoyloxy)butoxy]phosphonic acid (DAT-PA$_8$): Using the general procedure (III), starting from compound **7** (130 mg, 0.179 mmol) compound DAT-PA$_8$ (73 mg, 90%) was isolated as colorless oil. $[\alpha]^{20}_D$ = -12.6 (c 0.1, EtOH); ^{1}H NMR (400 MHz, $CDCl_3$): δ_{ppm} 5.26-5.19 (br s, 2H), 4.36-4.15 (br s, 4H), 2.29 (m, 4H), 1.55 (m, 4H), 1.23 (br s, 16H), 0.83 (m, 6H); ^{13}C NMR (100 MHz, $CDCl_3$): δ_{ppm} 176.7, 174.2, 71.2, 69.4, 67.4, 63.3, 34.2, 31.9, 29.8, 29.3, 29.1, 25.1, 24.9, 22.8, 14.2; ^{31}P NMR (161.9 MHz, $CDCl_3$): δ_{ppm} 1.09; HRMS (ESI) Calcd for $C_{20}H_{39}O_9PNa^+$ $[M+Na]^+$: 477.2229, Found: 477.2230.

(((4S,5S)-5-((benzyloxy)methyl)-2,2-dimethyl-1,3dioxolan-4-yl)methoxy)(*tert*-butyl) diphenylsilane (8): Colourless oil. $[\alpha]^{20}_D$ = -14.3 (c 0.1, CH_2Cl_2); ^{1}H NMR (400 MHz, $CDCl_3$): δ_{ppm} 7.68-7.63 (m, 5H), 7.44-7.28 (m, 10H), 4.59 (dd, 2H, J = 12.0 Hz, J = 12.0 Hz), 4.26-4.21 (m, 1H), 3.92-3.88 (m, 1H), 3.81-3.73 (m, 2H), 3.67-3.63 (m, 1H), 3.60-3.56 (m, 1H), 1.43 (s, 3H), 1.41 (s, 3H), 1.03 (s, 9H); ^{13}C NMR (100 MHz, $CDCl_3$): δ_{ppm} 138.2, 135.7, 133.2, 129.9, 128.5, 127.8, 127.7, 109.5, 78.4, 76.9, 73.6, 71.1, 64.3, 27.3, 27.1, 26.9, 19.3; HRMS (ESI) Calcd for $C_{30}H_{38}O_4SiNa^+$ $[M+Na]^+$: 513.2437, Found: 513.2439.

[(2S,3S)-4-(benzyloxy)-2,3-dihydroxybutoxy](tert-butyl)diphenylsilane (9): Using the general procedure (I), starting from compound **8** (550 mg, 1.12 mmol) compound **9** (429 mg, 85%) was isolated as colorless oil. $[\alpha]^{20}_D$ = -26.7 (c 0.2, CH_2Cl_2); ^{1}H NMR (400 MHz, $CDCl_3$): δ_{ppm} 7.60-7.55 (m, 5H), 7.35-7.14 (m, 10H), 4.41 (dd, 2H, J = 11.6 Hz, J = 11.2 Hz), 3.77-3.72 (m, 3H), 3.66-3.56 (m, 2H), 3.45-3.42 (m, 1H), 2.62 (br s, 2H), 0.97 (s, 9H); ^{13}C NMR (100 MHz, $CDCl_3$): δ_{ppm} 138.1, 135.8, 135.7, 135.0, 133.2, 130.1, 129.9, 128.6, 128.5, 128.1, 128.0, 127.8, 79.7, 72.8, 72.7, 71.9, 63.9, 26.9, 19.4, 19.3; HRMS (ESI) Calcd for $C_{27}H_{35}O_4Si$ $[M+H]^+$: 451.2305, Found: 451.2302.

(2S,3S)-4-(benzyloxy)-1-[(tert-butyldiphenylsilyl)oxy]-3-(octanoyloxy)butan-2-yl octanoate (10): Using the general procedure (II), starting from compound **9** (200 mg, 0.44 mmol) compound **10** (266 mg, 86%) was isolated as colorless oil; $[\alpha]^{20}_D$ = -11.3 (c 0.2, CH_2Cl_2); ^{1}H NMR (400 MHz, $CDCl_3$): δ_{ppm} 7.67-7.63 (m, 5H), 7.43-7.27 (m, 10H), 5.40-5.37 (m, 1H), 5.21-5.17 (m, 1H), 4.58 (dd, 2H, J = 12.0 Hz, J = 12.0 Hz), 4.35-4.26 (m, 1H), 4.19-4.12 (m, 1H), 3.83-3.66 (m, 2H), 2.29-2.20 (m, 4H), 1.58-1.55 (m, 4H), 1.26 (br s, 16H), 1.05 (s, 9H), 0.87 (t, 6H, J = 6.2 Hz); ^{13}C NMR (100 MHz, $CDCl_3$): δ_{ppm} 173.4, 173.0, 138.1, 135.8, 135.7, 135.6, 133.3, 133.2, 133.1, 129.9, 128.5, 128.0, 127.9, 78.0, 75.5, 73.2, 70.5, 62.7, 34.3, 34.2, 31.8, 29.2, 29.1, 26.9, 25.1, 25.0, 24.9, 22.7, 19.3, 19.2, 14.2; HRMS (ESI) Calcd for $C_{43}H_{63}O_6Si$ $[M+H]^+$: 703.4394, Found: 703.4398.

(2S,3S)-4-(benzyloxy)-1-hydroxy-3-(octanoyloxy)butan-2-yl octanoate (11): Using the general procedure (IV), starting from compound **10** (200 mg, 0.29 mmol) compound **11** (132 mg, 98%) was isolated as a colourless oil; $[\alpha]^{20}_D$ = -16.8 (c 0.1, CH_2Cl_2); ^{1}H NMR (400 MHz, $CDCl_3$): δ_{ppm} 7.37-7.27 (m, 5H), 4.63 (dd, 2H, J = 11.2 Hz, J = 11.6 Hz), 4.37-4.33 (m, 1H), 4.29-4.23 (m, 1H), 4.19-4.10 (m, 2H), 3.89 (m, 1H), 3.68-3.61 (m, 1H), 2.68 (br s, 1H), 2.36-2.24 (m, 4H), 1.63-1.28 (m, 4H), 1.28 (br s, 16H), 0.88 (t, 6H, J = 6.6 Hz), ^{13}C NMR (100 MHz, $CDCl_3$): δ_{ppm} 173.9, 173.7, 137.6, 128.6, 128.2, 76.4, 73.1, 69.6, 65.0, 62.7, 34.3, 34.2, 31.8, 29.2, 29.0, 25.0, 22.7, 14.2; HRMS (ESI) Calcd for $C_{27}H_{44}O_6Na^+$ $[M+Na]^+$: 487.3036, Found: 487.3036.

(2S,3S)-1-({[(2S)-2-amino-3-(benzyloxy)-3-oxopropoxy](benzyloxy)phosphoryl} oxy)-4-(benzyloxy)-3-(octanoyloxy)butan-2-yl octanoate (12): Using the general procedure (V), starting from *O*-benzyl *N,N,N′,N′*-tetraisopropyl phosphorodiamidite (109 mg 0.33 mmol), benzyl (S)-1-((benzyloxy)carbonyl)-2-hydroxyethylcarbamate (100 mg, 0.30 mmol) and compound **11** (139 mg, 0.30 mmol) compound **12** (235 mg, 83%) isolated as colourless oil ;; $[\alpha]^{20}_D$ = -15.1 (c 0.1, EtOH); ^{1}H NMR (400 MHz, $CDCl_3$): δ_{ppm} 7.33-7.25 (m, 20H), 6.00 (d, 1H, J = 7.2 Hz), 5.36-5.32 (m, 1H), 5.27-5.23 (m, 1H), 5.19 (s, 2H), 5.09 (s, 2H), 5.02-4.94 (m, 2H), 4.49-4.41 (m, 3H), 4.18-4.14 (m, 1H), 4.09-4.04 (m, 1H), 3.95 (dd, 2H, J = 11.2 Hz, J = 11.2 Hz), 3.55-3.48 (m, 2H), 2.33-2.20 (m, 4H), 1.63-1.52 (m, 4H), 1.26 (br s, 16 H), 0.87 (m, 6H); ^{13}C NMR (100 MHz, $CDCl_3$): δ_{ppm} 173.2, 173.0, 170.8, 156.7, 137.8, 136.5, 135.8, 135.6, 128.8, 128.7, 128.6, 128.3, 128.2, 128.0, 127.9, 127.7, 73.5, 70.3, 70.1, 69.8, 68.1, 67.5, 67.3, 66.2, 63.2, 56.6, 34.4, 34.3, 31.9, 29.9, 29.3, 29.2, 25.1, 22.8, 22.7, 14.3; ^{31}P NMR (161.9 MHz, $CDCl_3$): δ_{ppm} 0.17; HRMS (ESI) Calcd for $C_{52}H_{68}NO_{13}PNa^+$$[M+Na]^+$: 968.4326, Found: 968.4326.

(2S)-2-amino-3-({hydroxy[(2S,3S)-4-hydroxy-2,3-bis(octanoyloxy)butoxy] phosphoryl}oxy) propanoic acid (DAT-PS$_8$): Using the general procedure (III), starting from compound **12** (136 mg, 0.14 mmol) compound DAT-PS$_8$ (70 mg, 90%) was isolated as a yellow oil; $[\alpha]^{20}_D$ = -25.7 (c 0.1, EtOH); ^{1}H NMR (400 MHz, $CDCl_3$ + DMSO-d$_6$): δ_{ppm} 5.66 (d, 1H, J = 8.4 Hz), 4.86-4.82 (m, 1H), 4.00-3.90 (m, 2H), 3.84-3.80 (m, 1H), 3.74-3.70 (m, 1H), 3.62 (dd, 2H, J = 3.6 Hz, J = 3.6 Hz),

3.50-3.44 (m, 1H), 2.10 (t, 2H, J = 7.4 Hz), 1.97 (t, 2H, J = 7.6 Hz), 1.33-1.26 (m, 4H), 0.96 (br s, 16H), 0.56 (t, 6H, J = 6.8 Hz); ^{13}C NMR (100 MHz, $CDCl_3$ + DMSO-d_6): δ_{ppm} 173.0, 172.7, 79.2, 74.1, 70.3, 65.2, 62.7, 62.5, 55.6, 34.1, 33.9, 31.4, 30.6, 29.5, 28.8, 28.7, 28.2, 26.0, 25.1, 24.8, 24.6, 22.4, 14.0; ^{31}P NMR (161.9 MHz, $CDCl_3$): δ_{ppm} 0.04; HRMS (ESI) Calcd for $C_{23}H_{45}NO_{11}P$ $[M+H]^+$: 542.2730, Found: 542.2731.

(2S,3S)-4-(benzyloxy)-1-{[(benzyloxy)[(2-phenyl-1,3-dioxolan-4-yl)methoxy] phosphoryl]oxy }-3-(octanoyloxy)butan-2-yl octanoate (13): Using the general procedure (V), starting from compound **11** (150 mg, 0.32 mmol) compound **13** (212 mg, 83%) was isolated as a yellow oil; $[\alpha]^{20}_D$ = -23.1 (c 0.1, CH_2Cl_2); ^{1}H NMR (400 MHz, $CDCl_3$): δ_{ppm} 7.64-7.51 (m, 5H), 7.46-7.26 (m, 10H), 6.15 (s, 1H), 5.00-4.95 (m, 2H), 4.88-4.83 (m, 2H), 4.69 (s, 2H), 4.66-4.55 (m, 1H), 4.35-4.25 (m, 5H), 4.17-4.14 (m, 1H), 3.91-3.88 (m, 1H), 3.69-3.66 (m, 1H), 2.33-2.27 (m, 4H), 1.63-1.60 (m, 4H), 1.28 (br s, 16H), 0.88 (t, 6H, J = 6.4 Hz); ^{13}C NMR (100 MHz, $CDCl_3$): δ_{ppm} 174.1, 171.9, 135.6, 135.3, 134.7, 130.3, 130.1, 129.2, 128.7, 128.6, 128.5, 128.3, 127.8, 127.4, 127.2, 106.9, 76.3, 73.2, 72.2, 69.7, 65.4, 65.0, 62.7, 62.4, 62.3, 34.3, 34.2, 31.8, 31.1, 29.8, 29.2, 29.1, 25.0, 24.1, 22.7, 14.3, 14.2; ^{31}P NMR (161.9 MHz, $CDCl_3$): δ_{ppm} 1.52, 1.06; HRMS (ESI) Calcd for $C_{44}H_{61}O_{11}P$ $[M+H]^+$: 797.4030, Found: 797.4031.

(2,3-dihydroxypropoxy)[(2S,3S)-4-hydroxy-2,3-bis(octanoyloxy)butoxy] phosphinic acid (DAT-PG$_8$): Using the general procedure (III), starting from compound **13** (136 mg, 0.17 mmol) compound DAT-PG$_8$ (81 mg, 90%) was isolated as a yellow oil. $[\alpha]^{20}_D$ = -25.7 (c 0.1 EtOH); ^{1}H NMR (400 MHz, $CDCl_3$): δ_{ppm} 7.14 (br s, 1H), 5.20-5.16 (m, 2H), 4.33-4.25 (m, 2H), 4.18-4.13 (m, 1H), 4.06-4.02 (m, 1H), 3.94-3.88 (m, 2H), 3.80-3.76 (m, 1H), 3.70-3.65 (m, 2H), 3.48 (br s, 1H), 2.42-2.28 (m, 4H), 1.97-1.71 (m, 4H), 1.26 (br s, 16H), 0.88 (t, 6H, J = 6.6 Hz), ^{13}C NMR (100 MHz, $CDCl_3$): δ_{ppm} 173.5, 173.4, 74.5, 70.7, 65.6, 62.9, 55.8, 49.9, 35.9, 34.2, 32.8, 32.1, 31.8, 31.0, 29.8, 29.6, 29.6, 29.5, 29.4, 29.2, 29.1, 29.0, 26.4, 26.2, 25.6, 25.4, 25.0, 24.9, 22.8, 22.7, 14.2, 14.1; ^{31}P NMR (161.9 MHz, $CDCl_3$): δ_{ppm} 6.06, 0.15; HRMS (ESI) Calcd for $C_{23}H_{45}O_{11}P$ $[M+Na]^+$: 551.2597, Found: 551.2598.

Extent of Membrane Localization: The extent of localization of the ligands at the liposome interface was studied by NBD fluorescence quenching method, using PC/Ligand$_{16}$/NBD-PE liposomes (44.5/44.5/10/1) in 50 mM Tris buffer, pH 8.2, containing 150 mM NaCl, according to the reported procedure.[33, 34]

Protein Purification: The PKCα-C1a (homo sapiens), PKCδ-C1b (homo sapiens) and PKCθ-C1b (mus musculus) subdomains were expressed in *E. Coli* as a GST-tagged protein, purified by glutathione sepharose column and the GST tag was removed by the thrombin treatment using methods similar to those reported earlier.[25, 26, 33, 34, 45] The amino acid sequence of the C1 domains used for protein expression are shown in Figure 7.

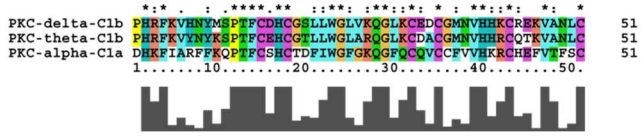

Figure 7: Sequences of the PKCα-C1a, PKCδ-C1b and PKCθ-C1b subdomains were aligned using CLUSTALX2 software.

Fluorescence Measurements: To calculate the binding parameters under membrane free system, ligand-induced Trp fluorescence quenching measurements were performed on a Fluoromax-4 spectrofluorometer at room temperature. The stock solutions of compounds were freshly prepared by first dissolving complexes in spectroscopic-grade dimethylsulfoxide (DMSO) and then diluted with buffer. The amount of DMSO was kept less than 3% (by volume) for each set of experiment and had no effect on any experimental results. For fluorescence titration, protein (1 μM) and varying concentration of ligands were incubated in a buffer solution (20 mM Tris, 150 mM NaCl, 50 μM $ZnSO_4$, pH 7.4) at room temperature. Protein was excited at 280 nm, and emission spectra were recorded from 300 to 550 nm. Proper background corrections were made to avoid the contribution of buffer and dilution effect. The resulting plot of Trp fluorescence as a function of ligand concentration was subject to nonlinear least-squares best-fit analysis to calculate the apparent dissociation constant for ligands (K_D(ML)), using equation 1, which describes binding to a single independent site.

$$(F_0 - F) = \Delta F_{\max}\left(\frac{[x]}{[x]+K_D(\mathrm{ML})}\right) + C \quad (1)$$

Where, F and F_0 represented the fluorescence intensity at 340 nm in the presence and the absence of ligand respectively. The ΔF_{max} represents the calculated maximal fluorescence change; $[x]$ represents the total monomeric ligand concentration.

Fluorescence anisotropy measurements were also performed on the same fluorimeter using similar methods described earlier. All anisotropy values of the proteins in the absence or presences of compounds are the mean values of three individual determinations.[33, 46] The degree (r) of anisotropy in the tryptophan fluorescence of the proteins was calculated using equation 2, at the peak of the protein fluorescence spectrum, where I_{VV} and I_{VH} are the fluorescence intensities of the emitted light polarized parallel and perpendicular to the excited light, respectively, and $G = I_{VH}/I_{HH}$ is the instrumental grating factor.

$$r = \frac{(I_{VV} - GI_{VH})}{(I_{VV} + 2GI_{VH})} \quad (2)$$

The anisotropy DPH under liposomal environment was measured according to the reported procedure. The fluorescence probe DPH was incorporated into the Giant vesicles by adding the dye dissolved in THF (1 mM) to vesicles up to a final concentration of 1.25 μM. After 30 min of incubation at room temperature DPH fluorescence anisotropy was measured at 430 nm (excitation 355 nm). The concentration of compounds was 2.9 μM.

Analysis of protein-to-membrane FRET based binding assay was used to measure the binding affinity and specificity of the selected ligands under a liposomal environment.[33] In this assay, membrane-bound C1 domain was displaced from liposomes (PC/PE/dPE/Ligand$_{16/18}$ (75/15/5/5)) by the addition of the DAG$_8$. The vesicles composed of PC/PE/PS/dPE (60/15/20/5) and PC/PE/PS/dPE/DAT-**1a** (55/15/20/5/5) were used as control and

for DAT-**1a** lipid, respectively. The stock solution of DAG_8 was titrated into the sample containing C1 domain (1 μM) and excess liposome (100 μM total lipid) in a buffer solution (20 mM Tris, 150 mM NaCl, 50 μM $ZnSO_4$, pH 7.4) at room temperature. The competitive displacement of protein from the membrane was quantitated using protein-to-membrane FRET signal (λ_{ex} = 280 nm and λ_{em} = 505 nm). Control experiments were performed to measure the dilution effect under similar experimental condition and the increasing background emission arising from direct dPE excitation. Protein-to-membrane FRET signal values as a function of DAG_8 concentration were subjected to nonlinear least-squares-fit analysis using equation 3 to calculate apparent equilibrium inhibition constants ($K_I(DAG_8)_{app}$) for DAG_8. Where, $[x]$ represents the total DAG_8 concentration and ΔF_{max} represents the calculated maximal fluorescence change.

$$F = \Delta F_{\max}\left(1 - \frac{[x]}{[x] + K_I(\mathrm{DAG_8})_{\mathrm{app}}}\right) + C \quad (3)$$

The equilibrium dissociation constant ($K_D(L_{16})$) for the binding of the C1 domains to the ligand-associated liposomes was calculated from equation 4, using $K_D(ML)$ and $K_I(DAG_8)_{app}$ values. Where, $[L_{16}]_{free}$ is the free ligand concentration (2.63 ± 0.04 μM). During calculation, the ligand concentration in the liposome interior were ignored, because of their inaccessibility for the protein. Thus, the protein accesses about half of lipids in the liposomes. The ligand concentration was used excess relative to the protein. The free ligand concentration was calculated by assuming that most of the protein would bind to the liposome and equimolar amount of ligand can be subtracted from the accessible ligand.

$$K_I(DAG_8)_{app} = K_D(ML)\left(1 + \frac{[L]_{free}}{K_D(L)}\right) \quad (4)$$

Molecular modeling: Molecular docking modeling was performed using the crystal structure of PKCδ C1b (Protein Data Bank code: 1PTR)[31]. The generation of energy minimized three-dimensional structure of ligands and ligand-protein docking was performed using the similar methods described earlier.[28,29]

Acknowledgment

The authors acknowledge their sincere gratitude to the Department of Chemistry, Central Instrumentation Facility, Indian Institute of Technology Guwahati, India. The authors are also thankful to the CSIR (02(0090)/12/EMR-II) Govt. of India for financial support.

Notes and references

Department of Chemistry, Indian Institute of Technology Guwahati, Assam 781039, India. Fax: 03 61258 2350; Tel: 03 61258 2325; E-mail: dmanna@iitg.ernet.in

† Electronic Supplementary Information (ESI) available: Protein binding parameters, molecular docking analysis, copies of ^1H and ^{13}C NMR spectra. See DOI: 10.1039/b000000x/

‡ N.M. and S.P. contributed equally to this work.

1 M. J. Wakelam, *Biochim Biophys Acta*, 1998, **1436**, 117-126.
2 F. Battaini and D. Mochly-Rosen, *Pharmacol Res*, 2007, **55**, 461-466.
3 G. Boije Af Gennas, V. Talman, J. Yli-Kauhaluoma, R. K. Tuominen and E. Ekokoski, *Curr Top Med Chem*, 2011, **11**, 1370-1392.
4 A. C. Newton, *Chem Rev*, 2001, **101**, 2353-2364.
5 A. C. Newton and L. M. Keranen, *Biochemistry*, 1994, **33**, 6651-6658.
6 F. Colon-Gonzalez and M. G. Kazanietz, *Biochim Biophys Acta*, 2006, **1761**, 827-837.
7 Y. Nishizuka, *Science*, 1992, **258**, 607-614.
8 E. M. Griner and M. G. Kazanietz, *Nature Reviews Cancer*, 2007, **7**, 281-294.
9 S. G. Rhee, *Annu Rev Biochem*, 2001, **70**, 281-312.
10 A. C. Newton, *Annu Rev Biophys Biomol Struct*, 1993, **22**, 1-25.
11 M. Medkova and W. Cho, *Biochemistry*, 1998, **37**, 4892-4900.
12 R. V. Stahelin, *J Lipid Res*, 2009, **50 Suppl**, S299-304.
13 H. J. Mackay and C. J. Twelves, *Endocrine-Related Cancer*, 2003, **10**, 389-396.
14 S. Sanchez-Bautista, S. Corbalan-Garcia, A. Perez-Lara and J. C. Gomez-Fernandez, *Biophys J*, 2009, **96**, 3638-3647.
15 D. Manna, N. Bhardwaj, M. S. Vora, R. V. Stahelin, H. Lu and W. Cho, *J Biol Chem*, 2008, **283**, 26047-26058.
16 M. Mosior, E. S. Golini and R. M. Epand, *Proc Natl Acad Sci U S A*, 1996, **93**, 1907-1912.
17 B. Ananthanarayanan, R. V. Stahelin, M. A. Digman and W. Cho, *J Biol Chem*, 2003, **278**, 46886-46894.
18 R. V. Stahelin, M. A. Digman, M. Medkova, B. Ananthanarayanan, J. D. Rafter, H. R. Melowic and W. Cho, *J Biol Chem*, 2004, **279**, 29501-29512.
19 R. V. Stahelin, M. A. Digman, M. Medkova, B. Ananthanarayanan, H. R. Melowic, J. D. Rafter and W. Cho, *J Biol Chem*, 2005, **280**, 19784-19793.
20 D. R. Dries, L. L. Gallegos and A. C. Newton, *J Biol Chem*, 2007, **282**, 826-830.
21 D. R. Dries and A. C. Newton, *J Biol Chem*, 2008, **283**, 7885-7893.
22 G. van Meer, D. R. Voelker and G. W. Feigenson, *Nat Rev Mol Cell Biol*, 2008, **9**, 112-124.
23 J. M. Boon, T. N. Lambert, A. L. Sisson, A. P. Davis and B. D. Smith, *J Am Chem Soc*, 2003, **125**, 8195-8201.
24 R. V. Stahelin, K. F. Kong, S. Raha, W. Tian, H. R. Melowic, K. E. Ward, D. Murray, A. Altman and W. Cho, *J Biol Chem*, 2012, **287**, 30518-30528.
25 N. Mamidi, S. Gorai, R. Mukherjee and D. Manna, *Molecular Biosystems*, 2012, **8**, 1275-1285.
26 N. Mamidi, S. Gorai, B. Ravi and D. Manna, *Rsc Advances*, 2014, **4**, 21971-21978.
27 M. D. Smith, D. Gong, C. G. Sudhahar, J. C. Reno, R. V. Stahelin and M. D. Best, *Bioconjug Chem*, 2008, **19**, 1855-1863.
28 M. D. Smith, C. G. Sudhahar, D. Gong, R. V. Stahelin and M. D. Best, *Mol Biosyst*, 2009, **5**, 962-972.
29 S. Benzaria, B. Bienfait, K. Nacro, S. M. Wang, N. E. Lewin, M. Beheshti, P. M. Blumberg and V. E. Marquez, *Bioorganic & Medicinal Chemistry Letters*, 1998, **8**, 3403-3408.
30 A. L. Plant, *Langmuir*, 1999, **15**, 5128-5135.
31 N. Brose and C. Rosenmund, *Journal of Cell Science*, 2002, **115**, 4399-4411.

32 M. N. Hodgkin, T. R. Pettitt, A. Martin, R. H. Michell, A. J. Pemberton and M. J. Wakelam, *Trends Biochem Sci*, 1998, **23**, 200-204.
33 N. Mamidi, R. Borah, N. Sinha, C. Jana and D. Manna, *J Phys Chem B*, 2012, **116**, 10684-10692.
34 N. Mamidi, S. Gorai, J. Sahoo and D. Manna, *Chem Phys Lipids*, 2012, **165**, 320-330.
35 O. Raifman, S. Kolusheva, M. J. Comin, N. Kedei, N. E. Lewin, P. M. Blumberg, V. E. Marquez and R. Jelinek, *FEBS J*, 2010, **277**, 233-243.
36 G. G. Zhang, M. G. Kazanietz, P. M. Blumberg and J. H. Hurley, *Cell*, 1995, **81**, 917-924.
37 G. Boije af Gennas, V. Talman, O. Aitio, E. Ekokoski, M. Finel, R. K. Tuominen and J. Yli-Kauhaluoma, *J Med Chem*, 2009, **52**, 3969-3981.
38 P. M. Blumberg, N. Kedei, N. E. Lewin, D. Yang, G. Czifra, Y. Pu, M. L. Peach and V. E. Marquez, *Current Drug Targets*, 2008, **9**, 641-652.
39 P. Sanchez-Pinera, V. Micol, S. Corbalan-Garcia and J. C. Gomez-Fernandez, *Biochem J*, 1999, **337 (Pt 3)**, 387-395.
40 C. Marin-Vicente, J. C. Gomez-Fernandez and S. Corbalan-Garcia, *Mol Biol Cell*, 2005, **16**, 2848-2861.
41 A. Torrecillas, S. Corbalan-Garcia, A. de Godos and J. C. Gomez-Fernandez, *Biochemistry*, 2001, **40**, 15038-15046.
42 E. J. Bolen and J. J. Sando, *Biochemistry*, 1992, **31**, 5945-5951.
43 S. J. Alvis, I. M. Williamson, J. M. East and A. G. Lee, *Biophys J*, 2003, **85**, 3828-3838.
44 I. M. Williamson, S. J. Alvis, J. M. East and A. G. Lee, *Biophys J*, 2002, **83**, 2026-2038.
45 A. Majhi, G. M. Rahman, S. Panchal and J. Das, *Bioorganic & Medicinal Chemistry*, 2010, **18**, 1591-1598.
46 D. Talukdar, S. Panda, R. Borah and D. Manna, *J Phys Chem B*, 2014.